

University of Groningen

## Retrieval of atmospheric CH<sub>4</sub> vertical information from ground-based FTS near-infrared spectra

Zhou, Minqiang; Langerock, Bavo; Sha, Mahesh; Kumps, Nicolas; Hermans, Christian; Petri, Christof; Warneke, Thorsten; Chen, Huilin; Metzger, Jean-Marc; Kivi, Rigel

*Published in:*  
 Atmospheric Measurement Techniques

*DOI:*  
[10.5194/amt-12-6125-2019](https://doi.org/10.5194/amt-12-6125-2019)

**IMPORTANT NOTE: You are advised to consult the publisher's version (publisher's PDF) if you wish to cite from it. Please check the document version below.**

*Document Version*  
 Publisher's PDF, also known as Version of record

*Publication date:*  
 2019

[Link to publication in University of Groningen/UMCG research database](#)

*Citation for published version (APA):*

Zhou, M., Langerock, B., Sha, M., Kumps, N., Hermans, C., Petri, C., Warneke, T., Chen, H., Metzger, J.-M., Kivi, R., Heikkinen, P., Ramonet, M., & De Mazière, M. (2019). Retrieval of atmospheric CH<sub>4</sub> vertical information from ground-based FTS near-infrared spectra. *Atmospheric Measurement Techniques*, 12(11), 6125-6141. <https://doi.org/10.5194/amt-12-6125-2019>

### Copyright

Other than for strictly personal use, it is not permitted to download or to forward/distribute the text or part of it without the consent of the author(s) and/or copyright holder(s), unless the work is under an open content license (like Creative Commons).

The publication may also be distributed here under the terms of Article 25fa of the Dutch Copyright Act, indicated by the "Taverne" license. More information can be found on the University of Groningen website: <https://www.rug.nl/library/open-access/self-archiving-pure/taverne-amendment>.

### Take-down policy

If you believe that this document breaches copyright please contact us providing details, and we will remove access to the work immediately and investigate your claim.

Downloaded from the University of Groningen/UMCG research database (Pure): <http://www.rug.nl/research/portal>. For technical reasons the number of authors shown on this cover page is limited to 10 maximum.



# Retrieval of atmospheric CH<sub>4</sub> vertical information from ground-based FTS near-infrared spectra

Minqiang Zhou<sup>1</sup>, Bavo Langerock<sup>1</sup>, Mahesh Kumar Sha<sup>1</sup>, Nicolas Kumps<sup>1</sup>, Christian Hermans<sup>1</sup>, Christof Petri<sup>2</sup>, Thorsten Warneke<sup>2</sup>, Huilin Chen<sup>3</sup>, Jean-Marc Metzger<sup>4</sup>, Rigel Kivi<sup>5</sup>, Pauli Heikkinen<sup>5</sup>, Michel Ramonet<sup>6</sup>, and Martine De Mazière<sup>1</sup>

<sup>1</sup>Royal Belgian Institute for Space Aeronomy (BIRA-IASB), Brussels, Belgium

<sup>2</sup>Institute of Environmental Physics, University of Bremen, Bremen, Germany

<sup>3</sup>Centre for Isotope Research (CIO), Energy and Sustainability Research Institute Groningen (ESRIG), University of Groningen, Groningen, the Netherlands

<sup>4</sup>UMS 3365 – OSU Réunion, Université de La Réunion, Saint-Denis, Réunion, France

<sup>5</sup>Finnish Meteorological Institute, Space and Earth Observation Centre, Sodankylä, Finland

<sup>6</sup>Laboratoire des Sciences du Climat et de l'Environnement (LSCE/IPSL), UMR CEA-CNRS-UVSQ, Gif-sur-Yvette, France

**Correspondence:** Minqiang Zhou (minqiang.zhou@aeronomie.be)

Received: 11 March 2019 – Discussion started: 23 April 2019

Revised: 13 September 2019 – Accepted: 28 October 2019 – Published: 25 November 2019

**Abstract.** The Total Carbon Column Observing Network (TCCON) column-averaged dry air mole fraction of CH<sub>4</sub> ( $X_{\text{CH}_4}$ ) measurements have been widely used to validate satellite observations and to estimate model simulations. The GGG2014 code is the standard TCCON retrieval software used in performing a profile scaling retrieval. In order to obtain several vertical pieces of information in addition to the total column, in this study, the SFIT4 retrieval code is applied to retrieve the CH<sub>4</sub> mole fraction vertical profile from the Fourier transform spectrometer (FTS) spectrum at six sites (Ny-Ålesund, Sodankylä, Bialystok, Bremen, Orléans and St Denis) during the time period of 2016–2017. The retrieval strategy of the CH<sub>4</sub> profile retrieval from ground-based FTS near-infrared (NIR) spectra using the SFIT4 code (SFIT4NIR) is investigated. The degree of freedom for signal (DOFS) of the SFIT4NIR retrieval is about 2.4, with two distinct pieces of information in the troposphere and in the stratosphere. The averaging kernel and error budget of the SFIT4NIR retrieval are presented. The data accuracy and precision of the SFIT4NIR retrievals, including the total column and two partial columns (in the troposphere and stratosphere), are estimated by TCCON standard retrievals, ground-based in situ measurements, Atmospheric Chemistry Experiment – Fourier Transform Spectrometer (ACE-FTS) satellite observations, TCCON proxy data and AirCore and

aircraft measurements. By comparison against TCCON standard retrievals, it is found that the retrieval uncertainty of SFIT4NIR  $X_{\text{CH}_4}$  is similar to that of TCCON standard retrievals with systematic uncertainty within 0.35 % and random uncertainty of about 0.5 %. The tropospheric and stratospheric  $X_{\text{CH}_4}$  from SFIT4NIR retrievals are assessed by comparison with AirCore and aircraft measurements, and there is a  $1.0 \pm 0.3$  % overestimation in the SFIT4NIR tropospheric  $X_{\text{CH}_4}$  and a  $4.0 \pm 2.0$  % underestimation in the SFIT4NIR stratospheric  $X_{\text{CH}_4}$ , which are within the systematic uncertainties of SFIT4NIR-retrieved partial columns in the troposphere and stratosphere respectively.

## 1 Introduction

The Total Carbon Column Observing Network (TCCON) is an international network established in 2004 using ground-based Fourier transform spectrometer (FTS) spectrometers to record direct solar absorption spectra in the near-infrared (NIR) spectral range and to retrieve from these spectra total columns of atmospheric greenhouse gases, including methane (CH<sub>4</sub>; Wunch et al., 2011). Currently, there are about 25 TCCON sites around the world with a latitude coverage of 45° S to 80° N. The standard TCCON retrieval code

is GGG2014 (developed and maintained at JPL, NASA); it performs a profile scaling retrieval. TCCON provides the dry air total column-averaged mole fraction of CH<sub>4</sub> ( $X_{\text{CH}_4}$ ), which has been compared to and indirectly calibrated by the Infrastructure for the Measurement of the Europe Carbon Cycle (IMECC) profiles over the European TCCON stations, the high-performance instrumented airborne platform for environmental research (HIAPER) Pole-to-Pole Observations (HIPPO) profiles over the TCCON stations in North America, East Asia and Oceania and several AirCore profiles (Karion et al., 2010) over Lamont (USA). A scaling factor of  $0.977 \pm 0.002$  ( $1\sigma$ ) is applied to the retrieved  $X_{\text{CH}_4}$  values to correct for the systematic bias. As one fixed value of 0.977 is applied to all the TCCON sites, the site-to-site bias is not taken into account. It is assumed that the remaining systematic uncertainty of the TCCON  $X_{\text{CH}_4}$  products is within 0.2%. The random uncertainty of the  $X_{\text{CH}_4}$  retrieval is about 0.5% (Wunch et al., 2015). TCCON  $X_{\text{CH}_4}$  observations have relatively larger footprints compared to surface in situ measurements, and thus could provide flux information on a regional scale (Wunch et al., 2016). TCCON  $X_{\text{CH}_4}$  measurements are widely used to validate the satellite observations, e.g. the Scanning Imaging Absorption Spectrometer for Atmospheric Chartography (SCIAMACHY) and the Thermal And Near-infrared Sensor for carbon Observation Fourier-Transform Spectrometer (TANSO-FTS; Houweling et al., 2014; Dils et al., 2014; Zhou et al., 2016). In addition, the TCCON  $X_{\text{CH}_4}$  observations are also used to evaluate atmosphere chemistry transport model simulations (Saito et al., 2012; Fraser et al., 2013; Agustí-Panareda et al., 2017).

The concentration of atmospheric CH<sub>4</sub> remained almost constant from about 1995 to 2006. However, after 2007, the CH<sub>4</sub> concentration started to increase with an annual growth rate about  $0.7 \text{ ppb yr}^{-1}$  (Rigby et al., 2008). The CH<sub>4</sub> in the atmosphere is released from gas and oil, coal, landfills, ruminant animals, rice agriculture, biomass burning, wetlands and lakes. The CH<sub>4</sub> in the troposphere is removed mainly by oxidation with hydroxyl radicals (OH), partly by absorption in the soil and partly by reacting with chlorine radicals in the marine boundary layer. The CH<sub>4</sub> in the stratosphere is removed by oxidation with OH, chlorine atoms and excited oxygen atoms (IPCC, 2013). The mole fraction of CH<sub>4</sub> decreases rapidly with altitude above the tropopause due to a higher photolysis rate in the stratosphere (Ehhalt and Heidt, 1973). The separation of the tropospheric and stratospheric CH<sub>4</sub> partial columns helps us to better understand the atmospheric CH<sub>4</sub> variability and to comprehensively evaluate model simulations (Ostler et al., 2016; Saad et al., 2016; Wang et al., 2017). The seasonal variation of CH<sub>4</sub> in the troposphere is dominated by its source and sink as well as the horizontal transport, while the seasonal variation of CH<sub>4</sub> in the stratosphere is strongly affected by the Brewer–Dobson circulation, vertical transport, intertropical convergence zone movement and stratospheric chemical reactions. A proxy method to derive the tropospheric and stratospheric  $X_{\text{CH}_4}$

from the TCCON retrievals based on the known relationship between CH<sub>4</sub> and hydrogen fluoride (HF) or nitrous oxide (N<sub>2</sub>O) in the stratosphere has been demonstrated by Wang et al. (2014) and Saad et al. (2014). The N<sub>2</sub>O and HF total columns are also available in the TCCON standard products. An alternative CH<sub>4</sub> profile retrieval method has been provided by Tukiainen et al. (2016), using dimension reduction and the Markov-chain Monte Carlo statistical estimation.

In this study, the CH<sub>4</sub> profile retrieval from ground-based FTS near-infrared spectra using the SFIT4 code (named SFIT4NIR retrievals) is carried out at six sites (Ny-Ålesund, Sodankylä, Bialystok, Bremen, Orléans and St Denis) for measurements performed during the time period of 2016–2017 in the framework of the EU Readiness of ICOS for Necessities of integrated Global Observations (RINGO) project. The full-physics SFIT4 retrieval code is based on the optimal estimation method (Rodgers, 2000), which is an updated version of SFIT2 (Pougetchev et al., 1995) and commonly used in the Network for the Detection of Atmospheric Composition Change – the Infrared Working Group (NDACC-IRWG; De Mazière et al., 2018). The TCCON sites and the SFIT4NIR retrieval strategy are introduced in the next section. The objective behind this study is to retrieve vertical information of CH<sub>4</sub> from TCCON spectra. In Sect. 3 the difference in  $X_{\text{CH}_4}$  retrieved using the SFIT4NIR to the  $X_{\text{CH}_4}$  retrieved from the standard TCCON retrievals is investigated. The tropospheric and the stratospheric  $X_{\text{CH}_4}$  retrieved using the SFIT4NIR retrievals are compared with other available data sets, such as ground-based in situ measurements, Atmospheric Chemistry Experiment – Fourier Transform Spectrometer (ACE-FTS) satellite observations and TCCON proxy data. Furthermore, the comparison results from the SFIT4NIR retrievals relative to the AirCore and aircraft profiles are also discussed in this section. Finally, conclusions are drawn in Sect. 4.

## 2 Data and method

### 2.1 TCCON sites

The locations of the TCCON sites used in this study are listed in Table 1. All sites use a Bruker IFS 125HR instrument to record NIR spectra in the range of 5000–10 000  $\text{cm}^{-1}$  with a spectral resolution of  $0.02 \text{ cm}^{-1}$ . The TCCON spectra from all sites in the time period of 2016–2017 were transferred to BIRA-IASB. A DC correction is applied to remove the variation of the interferogram caused by the solar intensity variation due to the presence of clouds during measurement (Keppel-Aleks et al., 2007). A python code is developed to convert the TCCON spectra from the OPUS format to the SFIT4 readable format.

**Table 1.** The coordinates and the altitudes (m a.s.l.) of the TCCON FTS sites used in this study.

Site	Latitude	Longitude	Altitude (m a.s.l.)	Reference
Ny-Ålesund	78.9° N	11.9° E	20	Notholt et al. (2017)
Sodankylä	67.4° N	26.6° E	188	Kivi et al. (2014)
Bialystok	53.2° N	23.0° E	180	Deutscher et al. (2014)
Bremen	53.1° N	8.8° E	30	Notholt et al. (2014)
Orléans	48.0° N	2.1° E	130	Warneke et al. (2014)
St Denis (Reunion Island)	21.0° S	55.4° E	87	De Mazière et al. (2014)

**Table 2.** Lists of the most important parameters in the SFIT4NIR retrieval strategy.

Retrieval window (cm <sup>-1</sup> )	5996.45–6007.55
Interfering species	CO <sub>2</sub> , H <sub>2</sub> O
Spectroscopy	ATM
Regularization	Tikhonov $L_1$ with $\alpha = 1000$
A priori profile	WACCM v6 (fixed)
SNR	250
ILS	linear polynomial fitting

## 2.2 SFIT4NIR retrieval strategy

The SFIT4NIR retrieval strategy is investigated based on the TCCON spectra at St Denis (a humid site) using the SFIT4\_v9.4.4 retrieval code. After that, the optimized retrieval strategy is applied for other sites. The key parameters used in the SFIT4NIR retrieval are listed in Table 2. The atmospheric line list (ATM) used in the GGG2014 code (Toon, 2014) has also been used in the forward model of the SFIT4NIR. Linear polynomial fitting is applied to a time-domain ideal instrument line shape (ILS) and the parameters are retrieved simultaneously. The a priori ILS is set as the ideal ILS. Since the Bruker 125HR spectrometers exhibit excellent ILS stability, the retrieved ILS are very constant and the retrieved maximal variations for modulation efficiency (ME) amplitude are within 2 % at these six sites. A detailed description of the retrieval settings, the averaging kernel and the retrieval uncertainty are presented in Sect. 2.2.1–2.2.5.

### 2.2.1 Retrieval window

Three windows listed in Table 3 are used to retrieve CH<sub>4</sub> total column values using the GGG2014 code. All these retrieval windows were tested with SFIT4NIR retrieval. The typical transmittance and residual for the three windows are shown in Fig. 1. The root mean square (RMS) of the residual in Band 1 is largest due to a bad fitting of several strong H<sub>2</sub>O absorption lines. The RMS of the residual in Band 2 is the lowest and is slightly better than that in Band 3. As an example, the retrieved CH<sub>4</sub> total columns using these three bands on 30 July 2016 are shown in Fig. 2. A clearly artificial symmetric variation for Band 1 is seen, which is probably due

**Table 3.** The retrieval windows used in the GGG2014 code.

	Window (cm <sup>-1</sup> )	Width (cm <sup>-1</sup> )	Interfering species
Band 1	5781.0–5897.0	116.0	CO <sub>2</sub> , H <sub>2</sub> O, N <sub>2</sub> O
Band 2	5996.45–6007.55	11.1	CO <sub>2</sub> , H <sub>2</sub> O
Band 3	6007.0–6145.0	138.0	CO <sub>2</sub> , H <sub>2</sub> O

to a bad fitting of the spectra. The results from Band 2 and 3 are similar. The difference between the retrieved CH<sub>4</sub> total columns from Band 2 and 3 are within  $0.3 \pm 0.1$  %. As Band 2 has the best fitting, it is selected as the retrieval window for our SFIT4NIR retrieval.

### 2.2.2 A priori profile

According to the optimal estimation method (OEM; Rodgers, 2000), an a priori profile is used to initialize the iteration during a retrieval process. In this study, SFIT4NIR uses the mean of the monthly profiles between 1980 and 2020 from the Whole Atmosphere Community Climate Model (WACCM) version 6 as the a priori profiles for CH<sub>4</sub> and CO<sub>2</sub>, while an H<sub>2</sub>O a priori profile is derived from the 6-hourly NCEP reanalysis data because of its high variability in the atmosphere.

### 2.2.3 Regularization

The retrieved CH<sub>4</sub> profile can be written as

$$\mathbf{x}_{r,CH_4} = \mathbf{x}_{a,CH_4} + \mathbf{A}(\mathbf{x}_{t,CH_4} - \mathbf{x}_{a,CH_4}) + \boldsymbol{\varepsilon}, \quad (1)$$

$$\mathbf{A} = (\mathbf{K}^T \mathbf{S}_e^{-1} \mathbf{K} + \mathbf{S}_a^{-1})^{-1} \mathbf{K}^T \mathbf{S}_e^{-1} \mathbf{K}, \quad (2)$$

where  $\mathbf{x}_{a,CH_4}$ ,  $\mathbf{x}_{t,CH_4}$  and  $\mathbf{x}_{r,CH_4}$  are the a priori, true and retrieved CH<sub>4</sub> mole fraction profiles respectively.  $\mathbf{A}$  is the averaging kernel, representing the sensitivity of the retrieved CH<sub>4</sub> profile to the true atmosphere status. The trace of  $\mathbf{A}$  is the degree of freedom for signal (DOFS), indicating the number of individual vertical information derived from the retrieval.  $\mathbf{K}$  is the Jacobian matrix.  $\boldsymbol{\varepsilon}$  is the retrieval uncertainty.  $\mathbf{S}_a$  and  $\mathbf{S}_e$  are the a priori covariance matrix and the measurement covariance matrix respectively.  $\mathbf{S}_e$  is determined by the signal-to-noise ratio (SNR).  $\mathbf{S}_a^{-1}$  and  $\mathbf{S}_e^{-1}$  are the two key parameters to constrain the retrieved CH<sub>4</sub>, and to determine whether the

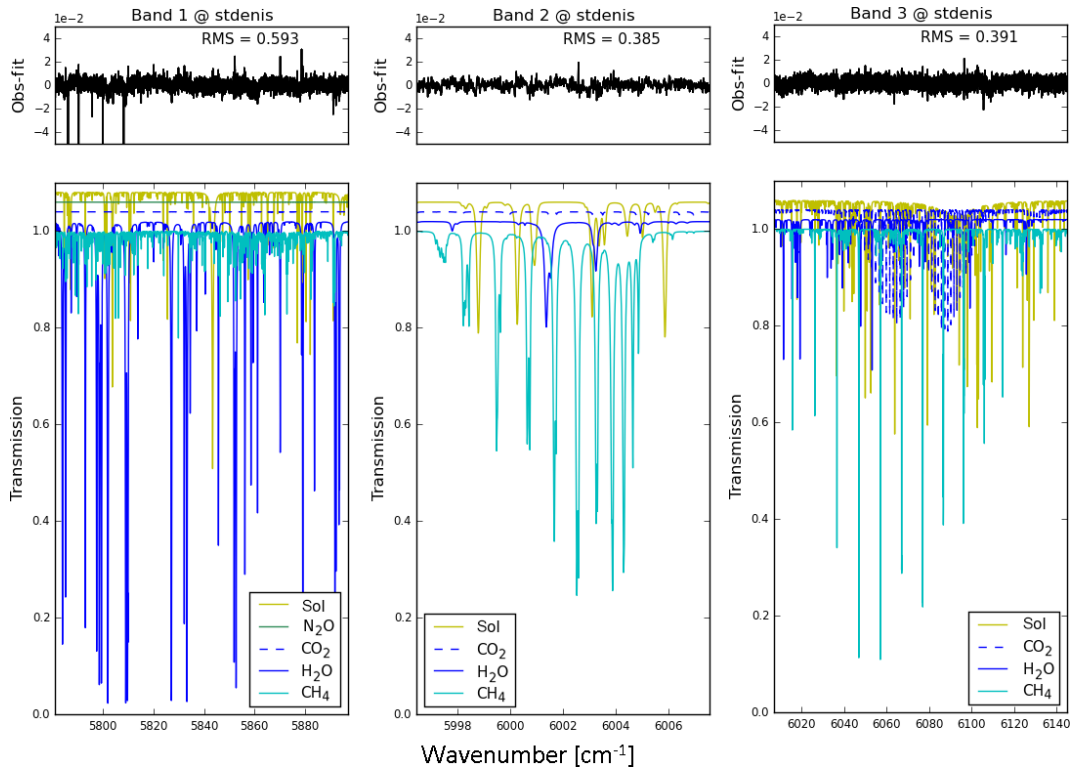


**Figure 1.** The transmittances of the species and solar lines in three bands from a typical spectrum at St Denis, together with the residual (observation–fitting). The transmittance of each component is shifted by 0.02 to better identify different species and the solar lines (sol).

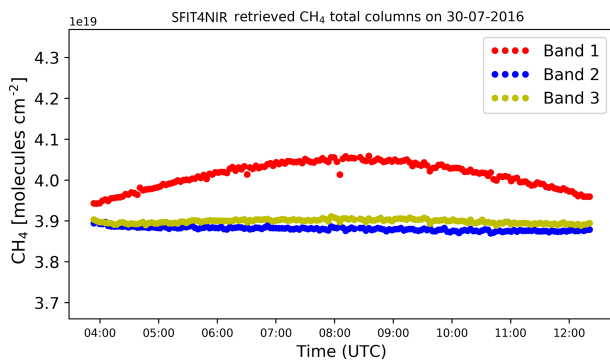


**Figure 2.** The SFIT4-retrieved CH<sub>4</sub> total columns using the three bands listed in Table 1 on 30 July 2016 (184 spectra).

retrieved CH<sub>4</sub> profile is mainly from the a priori information or from the measurement information. It is assumed that  $S_e$  is a diagonal matrix, where the diagonal elements are the inverse square of the SNR. The SNR of spectra is set to 250 at all the TCCON sites.  $S_a^{-1}$  is created using the Tikhonov  $L_1$  method (Tikhonov, 1963):

$$S_a^{-1} = \alpha L_1^T T L_1 \in \mathbf{R}^{(n,n)}, \quad (3)$$

$$\text{where } L_1 = \begin{bmatrix} -1 & 1 & 0 & \dots & 0 & 0 \\ 0 & -1 & 1 & \dots & 0 & 0 \\ \vdots & \vdots & \vdots & \ddots & \vdots & \vdots \\ 0 & 0 & 0 & \dots & -1 & 1 \end{bmatrix},$$

$T = \text{diag}(\Delta h^2)$ , where  $\Delta h$  is the thickness of each layer, and regularization strength  $\alpha$  is the key parameter to determine the correlation strength among layers.

The optimized  $\alpha$  value is chosen by extracting maximum possible information from the measurement while eliminating the artificial oscillation for the retrieved CH<sub>4</sub> profiles. Several  $\alpha$  values are tested using the spectra on 30 July 2016, and the RMS, DOFS and retrieved CH<sub>4</sub> total columns are listed in Table 4, along with the retrieved CH<sub>4</sub> vertical profiles in Fig. 3. The retrieved CH<sub>4</sub> profile shows a strong oscillation in the troposphere for  $\alpha = 100$ . The vertical profiles are similar for  $\alpha = 1000$  and  $\alpha = 10000$ , but they allow us to get a smaller RMS with  $\alpha = 1000$ . In summary, a regularization strength ( $\alpha$ ) of 1000 with the DOFS of about 2.4 is selected as the best choice for the SFIT4NIR retrieval.

#### 2.2.4 Averaging kernel

The left panel in Fig. 4 shows the typical averaging kernel (AVK) of SFIT4NIR retrieval with a solar zenith angle (SZA) of 63° at St Denis. The retrieved CH<sub>4</sub> profile is sensitive to the altitude range from the surface to the middle stratosphere

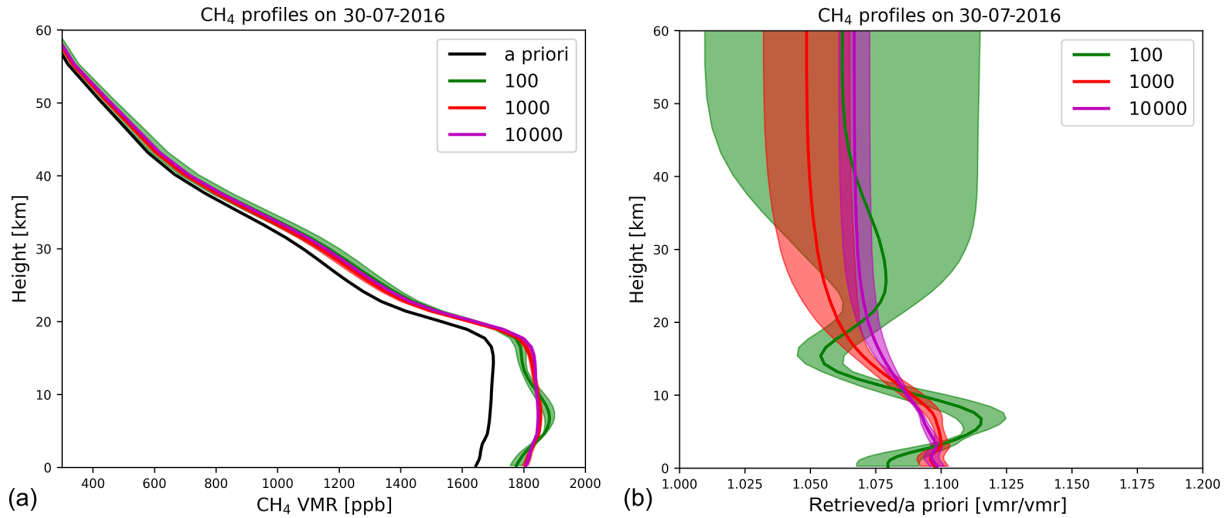


**Figure 3.** The SFIT4NIR a priori and the retrieved CH<sub>4</sub> vertical profiles (a), together with the ratios of the retrieved profiles to the a priori profile (b), with different regularization strength  $\alpha$  values.

**Table 4.** The mean and standard deviation of RMS, DOFS and retrieved CH<sub>4</sub> total columns from SFIT4NIR retrievals using different regularization strength  $\alpha$  values.

$\alpha$	100	1000	10000
RMS (%)	$0.34 \pm 0.06$	$0.34 \pm 0.06$	$0.35 \pm 0.06$
DOFS	$3.25 \pm 0.11$	$2.42 \pm 0.08$	$1.77 \pm 0.04$
Total column CH <sub>4</sub> ( $10^{18}$ molec. cm <sup>-2</sup> )	$38.62 \pm 0.05$	$38.64 \pm 0.04$	$38.65 \pm 0.04$

(about 40 km). The AVK shows that the SFIT4NIR-retrieved profile contains independent information in the troposphere and in the stratosphere (DOFS close to 1.0 for these two layers). In addition, the column-averaging kernels (right panel in Fig. 4) indicate that the retrieved CH<sub>4</sub> total column has a good sensitivity in the whole atmosphere, with a value close to 1.0 at all altitudes. The column-averaging kernels slightly vary with the SZAs, which is more constant than the AVK variability for the SZAs of the standard TCCON products (see Fig. 4 in Wunch et al., 2011).

### 2.2.5 Error budget

According to the OEM (Rodgers, 2000), the measurement uncertainty of the SFIT4NIR retrieval ( $\epsilon$  in Eq. 1) is estimated from three components: the smoothing error covariance matrix ( $\mathbf{S}_s$ ), the forward model parameter error covariance matrix ( $\mathbf{S}_f$ ) and the measurement error covariance matrix ( $\mathbf{S}_m$ ).

$$\mathbf{S}_s = (\mathbf{A} - \mathbf{I})\mathbf{S}_e(\mathbf{A} - \mathbf{I})^T, \quad (4)$$

$$\mathbf{S}_f = \mathbf{G}_y \mathbf{K}_b \mathbf{S}_b \mathbf{K}_b^T \mathbf{G}_y^T, \quad (5)$$

$$\mathbf{S}_m = \mathbf{G}_y \mathbf{S}_\epsilon \mathbf{G}_y^T, \quad (6)$$

where  $\mathbf{G}_y$  is the contribution matrix, representing the sensitivity of the retrieval to the measurement.  $\mathbf{S}_e$ ,  $\mathbf{S}_b$  and  $\mathbf{S}_\epsilon$  are the covariance matrices of the retrieval state vector, the forward model parameter and the measurement respectively. The retrieval state vector ( $\mathbf{x}$  in Eq. 1) not only includes the CH<sub>4</sub> vertical profile, but also includes the H<sub>2</sub>O and CO<sub>2</sub> columns, the slope of the background, the wavenumber shift and several ILS parameters. Each retrieved parameter has systematic and random uncertainties. The relative standard deviation of the CH<sub>4</sub> monthly means from the WACCM model in 1980–2020 is calculated as the random uncertainty of the CH<sub>4</sub> profile. For the systematic uncertainty, we have chosen a value of 5% (about 90 ppb in the troposphere), based on the difference between the a priori CH<sub>4</sub> mole fraction near the surface and the local in situ measurements (Zhou et al., 2018). As CH<sub>4</sub> is relatively stable in the atmosphere with a lifetime of  $\sim 9$  years, it is assumed that 5% systematic uncertainty is acceptable for all altitudes. The systematic and the random uncertainties for H<sub>2</sub>O and CO<sub>2</sub> are set to 5%. The systematic and random uncertainties of ILS parameters are set to 1%. The other retrieved parameters do not contribute significantly to the CH<sub>4</sub> uncertainty. The smoothing error in Table 5 represents the uncertainty contribution from the CH<sub>4</sub> vertical profile, while the errors from the retrieved parameters in Table 5 include the contribution from the H<sub>2</sub>O and CO<sub>2</sub> columns, the slope of the background, the wavenumber shift and several ILS parameters. The spectroscopy, the temperature and the SZA are the most

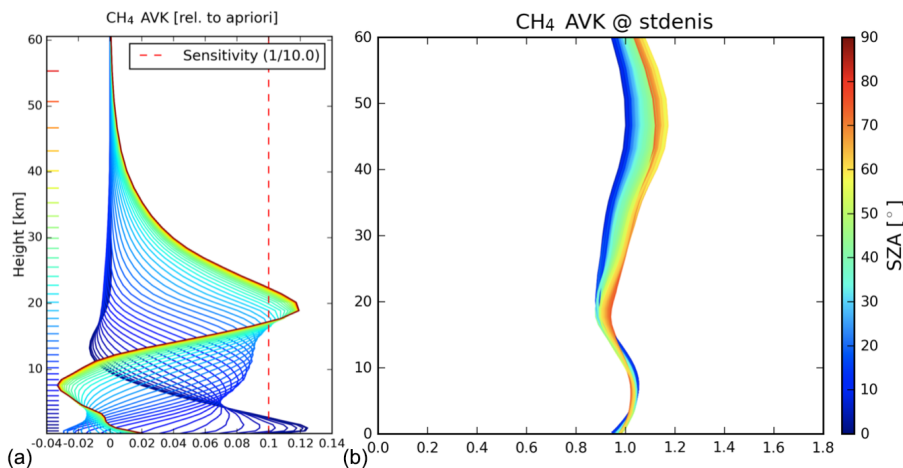


**Figure 4.** (a) A typical CH<sub>4</sub> averaging kernel matrix of the SFIT4NIR retrieval with the SZA of 63° at St Denis, in units of the mole fraction profile with respect to the a priori. (b) CH<sub>4</sub> column-averaging kernels (in unit of 1; applying for the partial column profile) with different solar zenith angles.

important parameters contributing to the forward model. According to the HITRAN2012 (Rothman et al., 2013), the uncertainty of CH<sub>4</sub> absorption in the selected retrieval window is about 2%–5%. Therefore, the systematic uncertainty of the spectroscopy is set to 3%, and the random uncertainty of the spectroscopic data is assumed to be negligible. The systematic and random uncertainties are set to 1% for the temperature. The systematic uncertainty is set to 0.1% and the random uncertainty is set to 0.5% for the SZA.  $S_e$  is assumed to be diagonal where the diagonal elements are the inverse square of the SNR. The propagated uncertainties of the total column and the partial columns (troposphere and stratosphere) are listed in Table 5. The mean tropopause height above St Denis is about 16.5 km. The systematic and random uncertainties of the SFIT4NIR-retrieved CH<sub>4</sub> total column are 3.2% and 0.5% respectively. The dominating component of the systematic uncertainty comes from the spectroscopy. The uncertainties of the partial column in the troposphere are closer to those of the total column, while the uncertainties of the partial column in the stratosphere are relatively large.

### 3 Results and discussion

The retrieval strategy listed in Table 2 is applied for all six sites. In this section, the data quality of the SFIT4NIR retrievals is evaluated with TCCON standard retrievals, ground-based in situ measurements, ACE-FTS satellite remote sensing observations, TCCON proxy  $X_{CH_4}$  data and AirCore measurements.

#### 3.1 TCCON standard retrievals

According to Sect. 2.2.5, the random uncertainty of the SFIT4NIR total column is about 0.5%, which is close to that

of TCCON retrieval (Wunch et al., 2015). The systematic uncertainty of the SFIT4NIR total column is about 3.2%, where a large contribution is from the spectroscopy. To better understand the systematic uncertainty of the SFIT4NIR-retrieved total column, the SFIT4NIR  $X_{CH_4}$  at six sites in 2016–2017 is calculated and compared with TCCON standard products. The systematic uncertainty of the TCCON  $X_{CH_4}$  products is within 0.2%.

GGG2014 uses the ratio between CH<sub>4</sub> and O<sub>2</sub> total columns to calculate the  $X_{CH_4}$  (Yang et al., 2002), as the atmospheric O<sub>2</sub> mole fraction is relatively stable with the mole fraction of 0.2095:

$$X_{CH_4} = 0.2095 \text{ TC}_{CH_4} / \text{TC}_{O_2}. \quad (7)$$

The  $X_{CH_4}$  from the SFIT4NIR retrieval is calculated as

$$X_{CH_4} = \frac{\text{TC}_{CH_4}}{\text{TC}_{air}^{dry}} = \frac{\text{TC}_{CH_4}}{P_s / (g m_{air}^{dry}) - \text{TC}_{H_2O} (m_{H_2O} / m_{air}^{dry})}, \quad (8)$$

where  $\text{TC}_{air}^{dry}$  and  $\text{TC}_{H_2O}$  are total columns of dry air and H<sub>2</sub>O;  $P_s$  is the surface pressure;  $g$  is the total column-averaged gravitational acceleration;  $m_{H_2O}$  and  $m_{air}^{dry}$  are molecular masses of H<sub>2</sub>O and dry air respectively (Deutscher et al., 2010). The uncertainty of  $P_s$  is better than 0.1 hPa and the uncertainty of H<sub>2</sub>O column in the troposphere is about 5%–10%; as a result, the uncertainty of the dry air column is about 0.1%. The uncertainty of  $X_{CH_4}$  is the combination of the uncertainties of the total column of CH<sub>4</sub> and the dry air column, while the uncertainty of the dry air column is negligible compared to the uncertainty of the SFIT4NIR retrieval (see Table 5). The SFIT4NIR tropospheric and stratospheric  $X_{CH_4}$  can be calculated following Eq. (8) using the partial columns of CH<sub>4</sub> and dry air in the troposphere and in the stratosphere respectively. The tropopause height is calculated

**Table 5.** The systematic and random uncertainties for the SFIT4NIR-retrieved CH<sub>4</sub> total column, partial columns in the troposphere (0–16.5 km) and in the stratosphere (16.5–50 km). The uncertainties are shown in percentages (%). The empty field shows where the uncertainty is negligible, with a value of less than 0.1 %.

Error	Total column		Troposphere (0–16.5 km)		Stratosphere (16.5–50 km)	
	Systematic	Random	Systematic	Random	Systematic	Random
Smoothing	0.2	0.2	0.2	0.2	1.2	1.6
Measurement		0.1		0.1		0.9
Retrieved parameters	0.2	0.2	0.1	0.1	2.5	2.5
Temperature	1.1	0.4	1.0	0.4	1.8	0.5
Spectroscopy	3.1		3.1		6.0	
SZA	0.1	0.2	0.1	0.2	0.2	0.9
Total	3.2	0.5	3.1	0.5	6.8	3.3

individually for each SFIT4NIR retrieval using the temperature and pressure profiles from the NCEP 6-hourly reanalysis data. The tropopause height varies from site to site according to its latitude. The tropopause height is about 8–11 km at Ny-Ålesund and Sodankylä, 10–12 km at Bialystok, Bremen and Orléans and 16–17 km at St Denis.

Figure 5 shows the time series of the hourly means of  $X_{\text{CH}_4}$  from SFIT4NIR and TCCON retrievals and their differences for measurements performed in 2016–2017. The mean and standard deviation of the  $X_{\text{CH}_4}$  difference between SFIT4NIR and TCCON (SFIT4NIR–TCCON) at the six sites are in the range between –2.3 ppb (–0.14 %) and 2.5 ppb (0.15 %) and between 4.7 ppb (0.3 %) and 9.9 ppb (0.5 %). The standard deviations of the differences at all sites are within 0.5 %, which is consistent with the combined random uncertainties from SFIT4NIR and TCCON retrievals. The systematic bias between the SFIT4NIR- and TCCON-retrieved  $X_{\text{CH}_4}$  is much lower than 3.2 %, indicating that the systematic uncertainty of the SFIT4NIR total column from the spectroscopy (see Table 3) is overestimated. Since the systematic uncertainty of the TCCON  $X_{\text{CH}_4}$  retrieval is better than 0.2 %, it is inferred that the systematic uncertainty of the SFIT4NIR  $X_{\text{CH}_4}$  retrieval is within 0.35 %. Figure 6 shows the scatter plots of the  $X_{\text{CH}_4}$  retrievals from SFIT4NIR and TCCON at the six sites. The linear regression line (dashed red line) is very close to the one-to-one lines for all panels. The correlation coefficient is in the range between 0.76 and 0.94. No obvious seasonal variation is seen from Figs. 5 and 6.

### 3.2 In situ measurements

This section presents the comparison results between the ground-based in situ measurements at the individual sites and the tropospheric  $X_{\text{CH}_4}$  retrieved using SFIT4NIR. Ground-based in situ measurements are more sensitive to the local sources and sinks as compared to the FTS measurements. The Traînou tower at the Orléans site takes in situ measurements at four heights (180, 100, 50 and 5 m). The measure-

ments at 180 m are used here as they are less affected by the boundary layer (Schmidt et al., 2014). In situ measurements for the St Denis site are taken from the measurements taken at Maïdo (2155 m) located at about 20 km away from St Denis (Zhou et al., 2018). The in situ measurements at Maïdo are less affected by the surface, and CH<sub>4</sub> is well-mixed in the lower atmosphere with a lifetime of 8–10 years (Kirschke et al., 2013). Both ground-based in situ instruments at Orléans and Maïdo are calibrated frequently at the Laboratoire des Sciences du Climat et de l'Environnement (LSCE). The in situ measurements from other sites are not used in order to reduce the influence from the boundary layer.

Figure 7 shows the monthly means and standard deviations of the co-located ground-based in situ and the SFIT4NIR tropospheric  $X_{\text{CH}_4}$  hourly means at Orléans and St Denis in 2016. In general, the seasonal cycle from the in situ measurements is similar to the one from the SFIT4NIR tropospheric  $X_{\text{CH}_4}$  retrievals at these two sites. However, the in situ tower measurements (180 m) at Orléans are still influenced by the boundary layer, and several high spikes are observed in March, June and December 2016. The in situ measurements at Orléans are found to be about 36 ppb larger than the SFIT4NIR tropospheric  $X_{\text{CH}_4}$ . Schmidt et al. (2014) showed that the CH<sub>4</sub> mole fractions at the four layers of the Orléans tower measurements are decreasing with increasing altitude. There is a strong CH<sub>4</sub> anthropogenic emission around Orléans (European Commission, 2013), which remains mainly at the surface. This might explain the bias between the SFIT4NIR tropospheric  $X_{\text{CH}_4}$  and the in situ tower measurements at Orléans. The in situ measurements at St Denis are found to be about 24 ppb lower than the SFIT4NIR tropospheric  $X_{\text{CH}_4}$ . Zhou et al. (2018) pointed out that the air near the surface above St Denis (0–2 km) mainly comes from the Indian Ocean and partly from the southern African region, whereas the air mass in the middle and upper troposphere (4–12 km) mainly comes from Africa and South America. As CH<sub>4</sub> emission on land is much larger than that from the ocean, it is reasonable that SFIT4NIR tropospheric



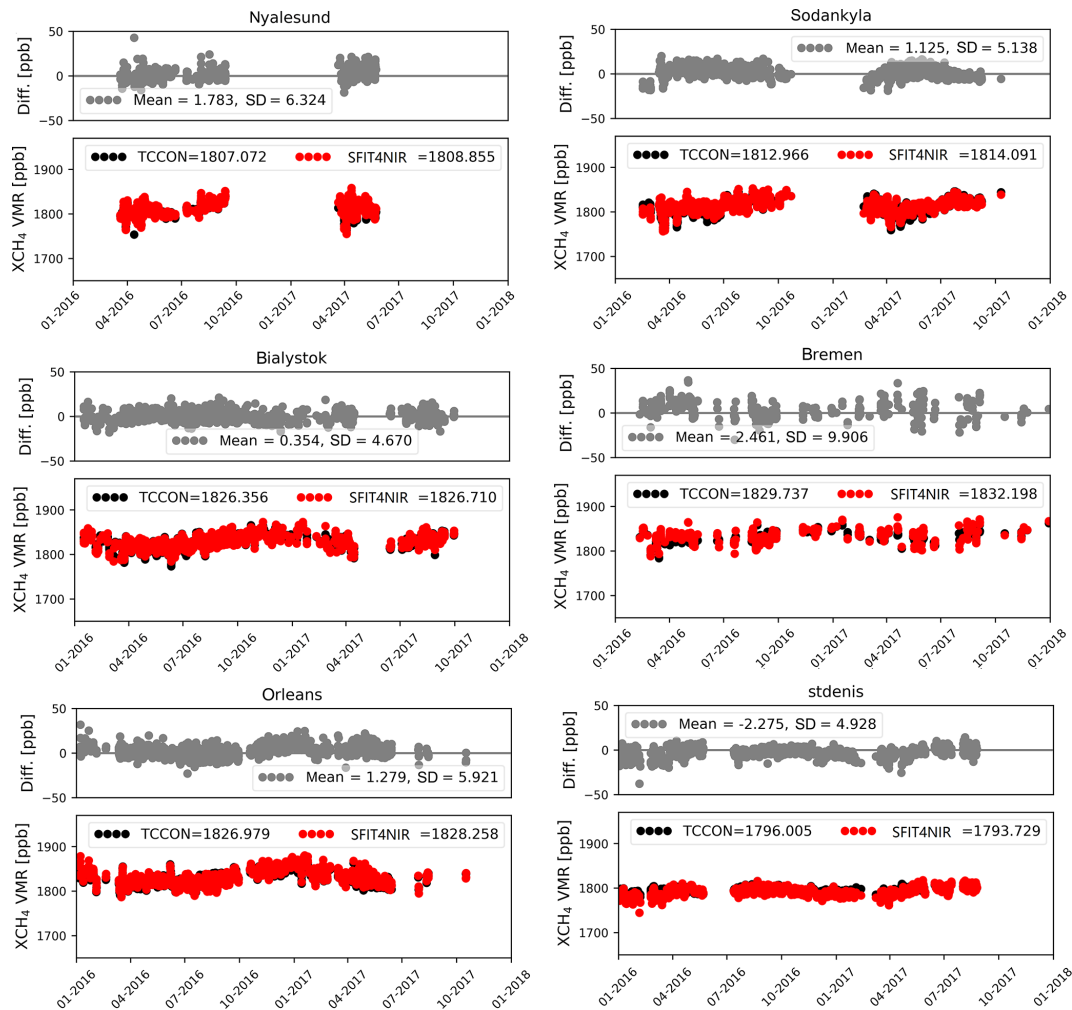


**Figure 5.** The time series of hourly means of  $X_{\text{CH}_4}$  from the SFIT4NIR and the TCCON retrievals at six TCCON sites during 2016–2017, together with their differences. For each site, the lower panel shows the time series of SFIT4NIR and TCCON measurements, and the upper panel shows the absolute difference between them (SFIT4NIR–TCCON; in ppb units). The values in the legend of the lower panel are the means of the TCCON and SFIT4NIR retrievals.

$X_{\text{CH}_4}$  is systematically larger than the CH<sub>4</sub> mole fraction at the surface.

The phases and amplitudes of the seasonal cycles from the SFIT4NIR tropospheric  $X_{\text{CH}_4}$  and the ground-based in situ CH<sub>4</sub> measurements are found to be in good agreement. CH<sub>4</sub> mole fraction is high in December–March and low in July–September at Orléans (located in the Northern Hemisphere), and high in July–September and low in December–March at St Denis (located in the Southern Hemisphere). The CH<sub>4</sub> seasonal variations in the troposphere are driven by the OH variation, which is the major sink of CH<sub>4</sub> in the atmosphere.

### 3.3 ACE-FTS satellite observations

The comparison results between the SFIT4NIR stratospheric  $X_{\text{CH}_4}$  and the ACE-FTS satellite observations are discussed in this section. The vertical range from the tropopause height

up to 50 km is treated as the stratosphere in this study. The ACE-FTS satellite has been monitoring the atmospheric CH<sub>4</sub> concentration mainly in the stratosphere since 2004 in solar occultation mode (Bernath et al., 2005). The latest level 2 version 3.6 data with data quality flag equal to 0 (without any known issues) are selected from the ACE/SCISAT data set (Sheese et al., 2015). The ACE-FTS CH<sub>4</sub> profile is retrieved at target altitudes with a vertical resolution of 3–4 km, and then it is interpolated onto a 1 km grid. The older version v2.2 data of the ACE-FTS CH<sub>4</sub> data have been compared to space-based satellite, balloon-borne and ground-based FTS data (De Maziere et al., 2008). The accuracy of the version 2.2 data is within 10 % in the upper troposphere–lower stratosphere, and within 25 % in the middle and higher stratosphere up to the lower mesosphere. The uncertainty of the new version of the ACE-FTS data has a reduction of about 10 % near

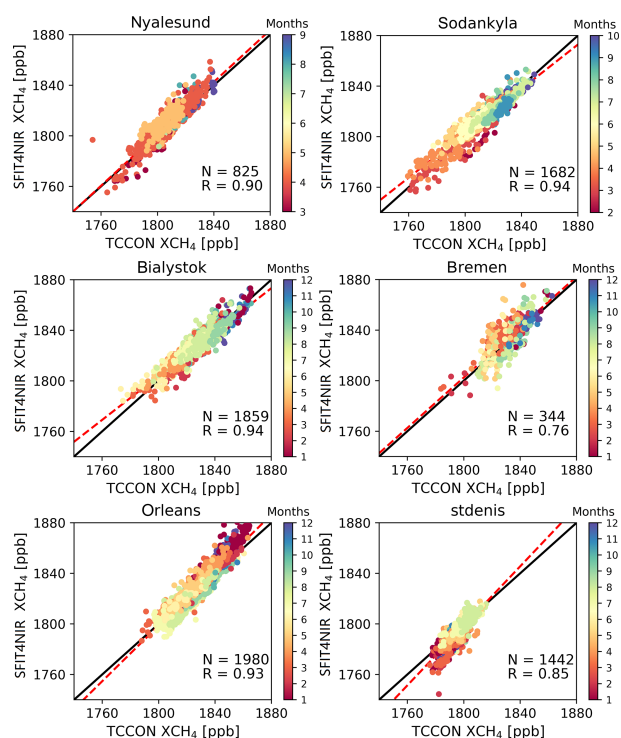


**Figure 6.** The scatter plots between SFIT4NIR and TCCON  $X_{\text{CH}_4}$  hourly retrievals at the six TCCON sites. The dots are coloured with the measurement months. In each panel, the black line is the one-to-one line and the dashed red line is the linear fitting.  $N$  is the measurement number and  $R$  is the correlation coefficient.

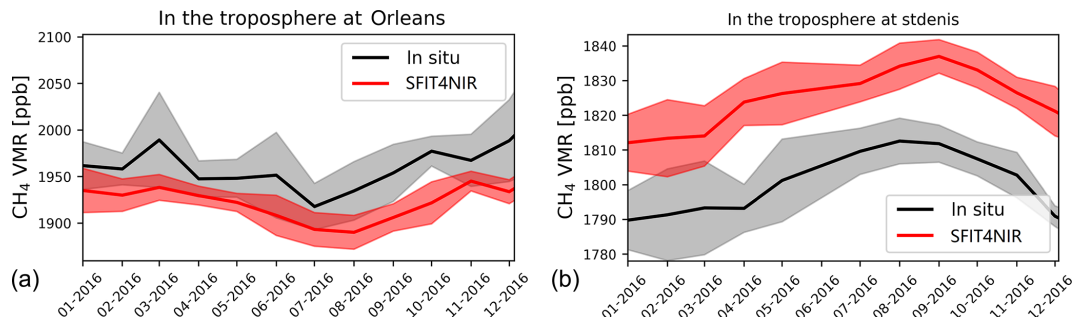
35–40 km and a slight reduction at 23 km (Waymark et al., 2014).

Figure 8 shows the SFIT4NIR and ACE-FTS co-located daily means of the stratospheric  $X_{\text{CH}_4}$  at Bialystok, Orleáns and St Denis. The ACE-FTS measurements are selected within  $\pm 3 \times 30^\circ$  (latitude by longitude) around each FTS site. Limited co-locations are found for Ny-Ålesund, Sodankylä and Bremen sites and so the results are not shown here. Figure 8 shows that the seasonal cycles (both phase and amplitude) of the stratospheric  $X_{\text{CH}_4}$  from SFIT4NIR and ACE-FTS are similar. The stratospheric  $X_{\text{CH}_4}$  shows a minimum in February–April and a maximum in August–October for the Bialystok and Orleáns sites located in the Northern Hemisphere, whereas the stratospheric  $X_{\text{CH}_4}$  shows a minimum in August–October and a maximum in February–April for the St Denis site, located in the Southern Hemisphere. The mean and the standard deviation of the differences in stratospheric  $X_{\text{CH}_4}$  between the SFIT4NIR and ACE-FTS measurements at these three sites are in the range between  $-0.27\%$  and  $2.06\%$  and between  $1.92\%$  and  $3.21\%$ , respectively, which are within their uncertainties.

### 3.4 TCCON proxy data

In this section, the tropospheric and stratospheric  $X_{\text{CH}_4}$  from SFIT4NIR retrievals are compared with the results derived from the  $\text{N}_2\text{O}$  and HF proxy methods at the six TCCON sites. We refer to Wang et al. (2014) and Saad et al. (2014) for the details of computing the tropospheric and stratospheric  $X_{\text{CH}_4}$  by the proxy retrieval method using  $\text{N}_2\text{O}$  and HF. Figure 9 shows the time series of the tropospheric and stratospheric  $X_{\text{CH}_4}$  from the TCCON proxy  $\text{N}_2\text{O}$  and HF method. First, the tropospheric and stratospheric  $X_{\text{CH}_4}$  from the  $\text{N}_2\text{O}$  and HF proxy methods are close to each other. However, a slight seasonal and site-dependent bias is observed. For example, the difference in the tropospheric  $X_{\text{CH}_4}$  between the  $\text{N}_2\text{O}$  proxy method and HF proxy method is larger in summer than that in winter at Ny-Ålesund. The tropospheric  $X_{\text{CH}_4}$  from the  $\text{N}_2\text{O}$  and HF proxy methods are very close to each other for St Denis, while for the other five sites, the tropospheric  $X_{\text{CH}_4}$  from the  $\text{N}_2\text{O}$  method is larger by about 15–20 ppb than the HF method. The bias in the tropospheric  $X_{\text{CH}_4}$  between the  $\text{N}_2\text{O}$  and HF methods is in a good agreement with Fig. 7 in Wang et al. (2014). As the TCCON  $\text{N}_2\text{O}$  retrievals are corrected to the WMO scale (Wunch et al., 2015), while HF retrievals have not been validated, the systematic bias is probably due to the uncertainty of the  $X_{\text{HF}}$  product. Second, at St Denis (a moist site), the TCCON HF retrievals are strongly affected by  $\text{H}_2\text{O}$  so that the TCCON proxy method tropospheric and the stratospheric  $X_{\text{CH}_4}$  data using HF have many outliers.

Figure 9 also shows the time series of the tropospheric and stratospheric  $X_{\text{CH}_4}$  from the SFIT4NIR retrievals. The SFIT4NIR tropospheric  $X_{\text{CH}_4}$  data are close to the proxy data at St Denis, while the SFIT4NIR tropospheric  $X_{\text{CH}_4}$  data are systematically larger than the results from the proxy method at the five sites located in the Northern Hemisphere. The vital difference between St Denis and other sites is that the tropopause height at St Denis is about 16.5 km, which is relatively higher than the tropopause height of 9–12 km at other sites. It seems that the partial column of  $\text{CH}_4$  from the SFIT4NIR retrieval is larger than that from the TCCON proxy data in the vertical range from surface to about 10 km, while it is smaller than that from the TCCON proxy data above 10 km. The bias in the vertical range from surface to 10 km might be able to be compensated by the part of 10–16.5 km, due to the relatively high tropopause height at St Denis. The phases of the  $X_{\text{CH}_4}$  seasonal variations from the SFIT4NIR retrievals are almost the same as those from the proxy method, while the amplitudes of the variations from the SFIT4NIR retrievals are larger than those from the proxy method in the tropospheric component. There are two possible explanations: (1) the proxy method assumes that the vertical mole fraction profile of HF or  $\text{N}_2\text{O}$  are constant in the troposphere, and the  $\text{CH}_4$  mole fraction in the upper troposphere is calculated as the tropospheric  $X_{\text{CH}_4}$  for the proxy method; (2) the tropopause height in the proxy method has a chemical definition, which differs from the tropopause height cal-



**Figure 7.** The time series of the monthly means (solid line) and standard deviations (shading) from the SFIT4NIR tropospheric  $X_{\text{CH}_4}$  and the ground-based in situ CH<sub>4</sub> measurements at Orléans (a) and at St Denis (b). At Orléans, the in situ measurements are recorded at 180 m on a tower at the same place. The in situ measurements at St Denis are recorded at 2155 m on Maïdo mountain, which is about 20 km away from St Denis.

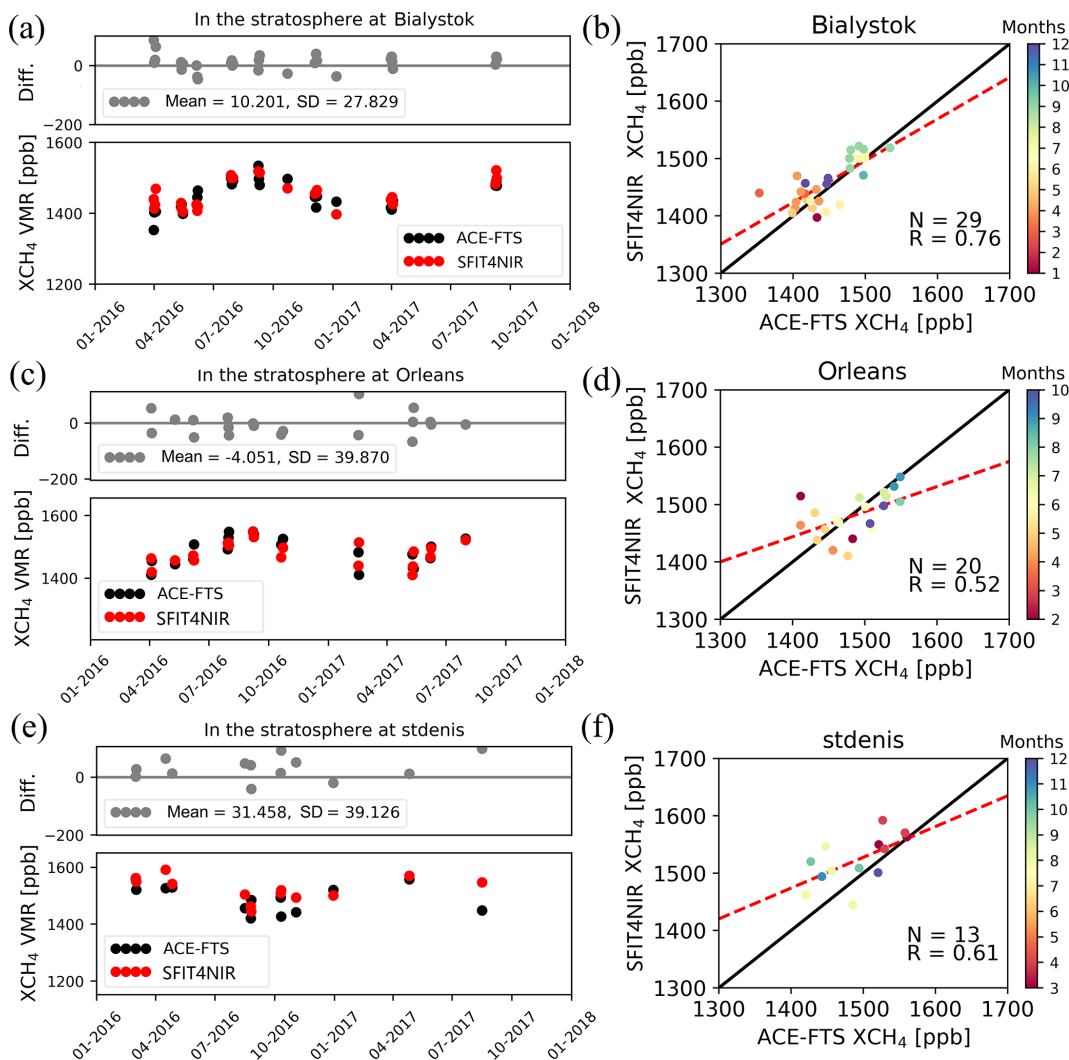


**Figure 8.** (a, c, e) The time series of the daily mean of the co-located SFIT4NIR and ACE-FTS stratospheric  $X_{\text{CH}_4}$  daily mean measurements, together with the absolute differences (unit: ppb) between them for Bialystok, Orléans and St Denis. (b, d, f) The correlation plots between the co-located SFIT4NIR and the ACE-FTS stratospheric  $X_{\text{CH}_4}$  daily means.

culated from the temperature and the altitude profiles (Wang et al., 2017).

### 3.5 AirCore measurements at Sodankylä

The AirCore is an atmospheric sampling system which uses a long tube to sample the air from the surrounding atmosphere and to preserve profiles of the trace gases of interest from the surface (few hundred metres) to the middle stratosphere (about 30 km; Karion et al., 2010). Regular AirCore measurements of CH<sub>4</sub> have been carried out at Sodankylä since September 2013. During 2016–2017, we selected seven AirCore profiles which are within 1 h of SFIT4NIR measurements.

As an example, the AirCore CH<sub>4</sub> profile on 5 September 2017, together with the co-located (within ± 1 h) a priori and retrieved SFIT4NIR profiles are shown in the left panel of Fig. 10. AirCore and FTS data cannot be compared directly, because the AirCore profile has a high vertical resolution but it covers only a part of the total column that is observed by the FTS. The AirCore measurement for this launch covers the vertical range from about 0.6 to 26 km, and needs to be extended for comparison with the FTS data. For the extrapolation, a scaled SFIT4NIR a priori profile is applied to extend the AirCore CH<sub>4</sub> profile above 26 km, and the local surface CH<sub>4</sub> mole fraction observations (Kilkkki et al., 2015) are applied to extend the AirCore CH<sub>4</sub> profile below 0.6 km. In order to take the vertical sensitivity of the FTS retrieval into account (Rodgers, 2003), the “extended” AirCore profile is then smoothed with the co-located SFIT4NIR retrieval

$$\mathbf{x}_{\text{aircore,s}} = \mathbf{x}_a + \mathbf{A}(\mathbf{x}_{\text{insitu}} - \mathbf{x}_a), \quad (9)$$

where  $\mathbf{x}_{\text{insitu}}$  is the “extended” AirCore profile,  $\mathbf{x}_a$  is the a priori profile of the SFIT4NIR retrieval and  $\mathbf{x}_{\text{aircore,s}}$  is the smoothed AirCore profile. The mean and the standard deviation of the relative differences between the co-located SFIT4NIR retrievals and the smoothed AirCore profile  $((\text{SFIT4NIR} - \text{AirCore}) / \text{AirCore} \times 100 \%)$  are shown in the right panel of Fig. 10. The bias is about +1.5 % in the lower and the middle troposphere, between +1 and −4 % in the upper troposphere and lower stratosphere region, and about −2.5 % in the middle and upper stratosphere.

Figure 11 shows the scatter plots of  $X_{\text{CH}_4}$  between the co-located SFIT4NIR retrievals and the AirCore measurements for the whole atmosphere, and for the tropospheric and stratospheric components. The error bars are the random uncertainties of the SFIT4NIR retrievals and the AirCore measurements. It is assumed that the random uncertainty of the AirCore profile is about 0.1 % between the surface and its maximum measurement altitude ( $\sim 30$  km), and it is about 2 % above the maximum measurement altitude. The slope of the regression line ( $a = 1.001$ ) in the whole atmosphere indicates that there is almost no systematic difference between the SFIT4NIR and the AirCore  $X_{\text{CH}_4}$ , which is consistent with the result in the comparison between SFIT4NIR and

TCCON  $X_{\text{CH}_4}$  measurements (Figs. 5 and 6). The SFIT4NIR tropospheric  $X_{\text{CH}_4}$  is about  $1.1 \pm 0.4 \%$  larger than the AirCore measurements and the SFIT4NIR stratospheric  $X_{\text{CH}_4}$  is about  $4.0 \pm 2.0 \%$  less than the AirCore measurements. These differences between the SFIT4NIR retrievals and AirCore measurements are within the systematic uncertainties of the SFIT4NIR partial columns in the troposphere and stratosphere, and it is inferred that the systematic uncertainty of the SFIT4NIR partial column mainly comes from the uncertainty of the spectroscopy (see Table 5).

### 3.6 Aircraft measurements during the IMECC campaign

The Infrastructure for Measurement of the European Carbon Cycle (IMECC) aircraft equipment passed over several European TCCON sites in September and October 2009, including Orléans, Bremen and Bialystok. We refer to Geibel et al. (2012) for a detail description of the IMECC aircraft data. The aircraft equipment cover a vertical range from about 300 to 13 000 m, mainly in the troposphere. Therefore, in this section, we use the co-located aircraft measurements for comparison with the SFIT4NIR tropospheric  $X_{\text{CH}_4}$ . The location, date and time of the overflight, SZA and the profile code are listed in Table 1 in Geibel et al. (2012). There are four aircraft vertical profiles over Bialystok (BI-OF1a, BI-OF1b, BI-OF2a, BI-OF2b), four profiles over Orléans (OR-OF1a, OR-OF1b, OR-OF2a, OR-OF2b) and two profiles over Bremen (BR-OF1a, BR-OF2a).

To compare the aircraft measurements with the SFIT4NIR, the aircraft profiles need to be extended for comparison with FTS retrievals. The extrapolation method is the same as described in Sect. 4.2 in Geibel et al. (2012). For the near-ground part, ground-based in situ data from the co-located tall-tower stations are used to extend the aircraft data to the ground at Orléans and Bialystok, and the values measured at the lowermost altitude by the aircraft are linearly extrapolated to the surface at Bremen. For the upper part, the TCCON (GGG2012) a priori profile multiplied by the retrieval scaling factor is used. The uncertainties of “extended” aircraft profiles have been shown in Table 2 in Geibel et al. (2012). After that, the “extended” aircraft profile is smoothed with FTS retrieval using Eq. (9), where the  $x_{\text{insitu}}$  is the aircraft measurement. The SFIT4NIR retrievals within a time window of ± 1 h around the aircraft overflight are chosen. The standard deviation of the co-located SFIT4NIR retrievals is used as the random uncertainty of the FTS retrieval.

The smoothed aircraft tropospheric  $X_{\text{CH}_4}$  is  $1.0 \pm 0.2 \%$  larger than the SFIT4NIR tropospheric  $X_{\text{CH}_4}$ , which is consistent with the result from the comparison between the AirCore measurements and SFIT4NIR retrievals ( $1.1 \pm 0.4 \%$ ). Combining the AirCore measurements at Sodankylä and aircraft measurements at Orléans, Bremen and Bialystok, Fig. 12 shows that there is a systematic overestimation of  $1.0 \pm 0.3 \%$  in the SFIT4NIR tropospheric  $X_{\text{CH}_4}$ . Further in-

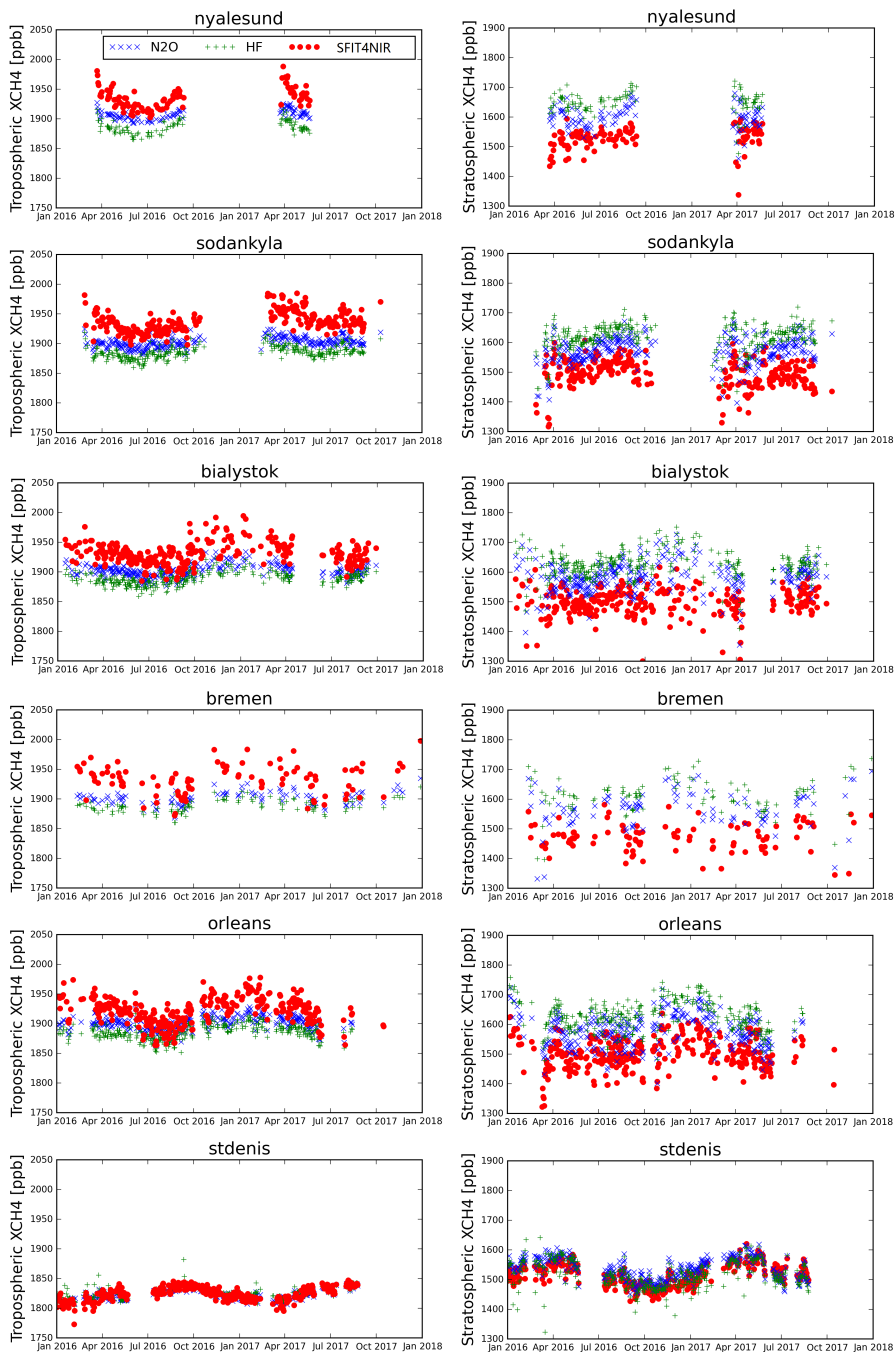


**Figure 9.** The time series of the tropospheric (left panels) and the stratospheric (right panels) co-located  $X_{\text{CH}_4}$  hourly means from the SFIT4NIR and the proxy method (both  $\text{N}_2\text{O}$  and HF) at the six TCCON sites.

vestigation is required to see if the systematic bias can be observed at other sites.

#### 4 Conclusions

The retrieval of  $\text{CH}_4$  vertical information from TCCON FTS NIR spectra has been carried out at six sites during 2016–

2017 using the SFIT4 code. The retrieval strategy of the SFIT4NIR has been discussed, including the spectroscopy, retrieval window, an a priori profile, SNR and regularization. The AVK shows that the SFIT4NIR-retrieved profile is sensitive to the altitude range from the surface to the middle stratosphere (about 40 km), and the column-averaging kernel has a good sensitivity in the whole atmosphere. The DOFS

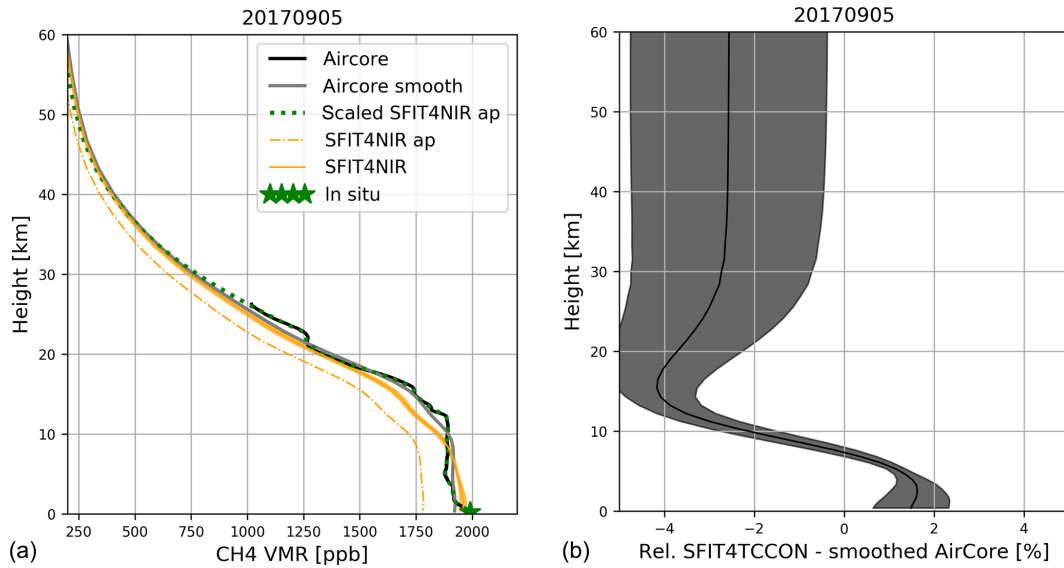


**Figure 10.** (a) The CH<sub>4</sub> profile from the AirCore measurement (solid black line) on 5 September 2017, together with the SFIT4NIR a priori (dash-dotted orange line) and retrieved (solid orange line) profiles. The AirCore measurement is extrapolated with the surface in situ measurements (green star) and the scaled SFIT4NIR a priori profile (dotted green line). The grey line is the smoothed AirCore profile. (b) The mean (solid black line) and the standard deviation (shading) of the relative difference between the co-located SFIT4NIR-retrieved profiles and the smoothed AirCore measurements ( $(\text{SFIT4NIR} - \text{AirCore}) / \text{AirCore} \times 100\%$ ).

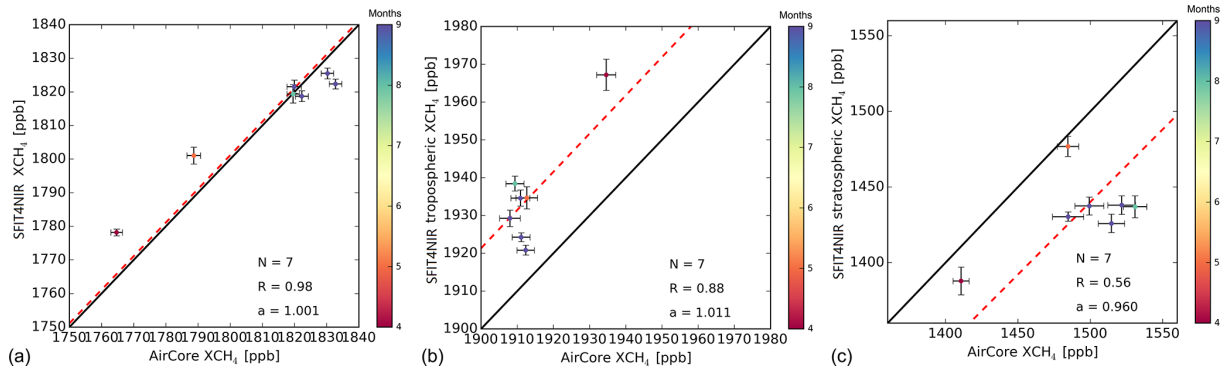


**Figure 11.** The scatter plots of  $X_{\text{CH}_4}$  between the SFIT4NIR and the AirCore measurements for the whole atmosphere (a), and for the tropospheric (b) and stratospheric (c) components. In each panel, the black line is the one-to-one line and the dashed red line is the regression line with the intercept to zero ( $y = a \cdot x$ ).  $N$  is the co-located measurement number,  $R$  is the correlation coefficient, and  $a$  is the slope.

of the SFIT4NIR is about 2.4, with two distinct pieces of information in the troposphere and the stratosphere. The systematic and random uncertainties of the SFIT4NIR-retrieved total column are about 3.2 % and 0.5 %.

The SFIT4NIR-retrieved CH<sub>4</sub> total columns and partial columns (troposphere and stratosphere) have been evaluated based on the standard TCCON retrievals, ground-based in situ measurements, ACE-FTS satellite observations, TCCON proxy  $X_{\text{CH}_4}$  data and AirCore measurements at Sodankylä. It is found that the SFIT4NIR-retrieved  $X_{\text{CH}_4}$  data are very close to the standard TCCON retrievals with the mean bias between  $-0.14\%$  and  $0.15\%$  and the standard deviation of bias between 0.3 % and 0.5 % at the six TCCON

sites. Additionally, there is no obvious seasonal variation in the difference between the SFIT4NIR and TCCON  $X_{\text{CH}_4}$  data. The SFIT4NIR tropospheric and stratospheric  $X_{\text{CH}_4}$  can observe the CH<sub>4</sub> seasonal variation very well, which has been confirmed by the ground-based in situ measurements and ACE-FTS observations respectively. The tropospheric and the stratospheric  $X_{\text{CH}_4}$  from SFIT4NIR retrievals have also been compared with the results from the TCCON proxy method. The phases of the seasonal cycles from SFIT4NIR retrievals and TCCON proxy data are consistent, though the amplitudes of the variations from the SFIT4NIR retrievals are relatively larger than those from the proxy method, especially in the troposphere. Further investigation is needed

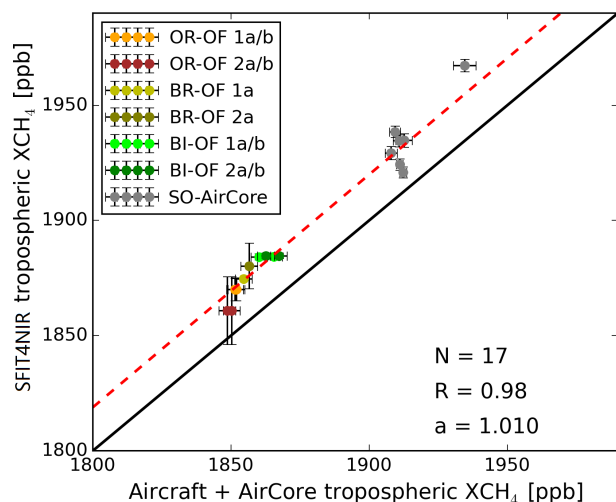


**Figure 12.** The scatter plots of  $X_{\text{CH}_4}$  between the SFIT4NIR and the IMECC aircraft measurements together with the AirCore measurements for the tropospheric components. The black line is the one-to-one line and the dashed red line is the regression line with the intercept to zero ( $y = a \cdot x$ ).  $N$  is the co-located measurement number,  $R$  is the correlation coefficient and  $a$  is the slope.

to understand the accuracy of the seasonal cycle from the SFIT4NIR tropospheric  $X_{\text{CH}_4}$  when more aircraft or AirCore measurements become available. By comparison against AirCore measurements at Sodankylä, it is found that there is almost no systematic bias between the SFIT4NIR and AirCore  $X_{\text{CH}_4}$  (in the whole atmosphere), which is consistent with the comparison between the SFIT4NIR and the TCCON standard retrievals. An underestimation of  $4.0 \pm 2.0 \%$  in the SFIT4NIR stratospheric  $X_{\text{CH}_4}$  is seen by comparison with AirCore measurements, and an overestimation of  $1.0 \pm 0.3 \%$  in the SFIT4NIR tropospheric  $X_{\text{CH}_4}$  is seen by comparing it with AirCore measurements and IMECC aircraft measurements. These biases are within the systematic uncertainties of SFIT4NIR-retrieved partial columns in the troposphere and stratosphere respectively.

**Data availability.** The TCCON data are publicly available through the TCCON wiki (<https://tccondata.org/>, last access: 12 September 2019). The ACE-FTS data used in this study are available from <https://ace.uwaterloo.ca/data.php> (last access: 20 November 2019) (registration required). The SFIT4NIR retrievals, TCCON proxy data, ground-based in situ measurements and AirCore measurements are available by contacting the author.

**Author contributions.** MZ wrote the manuscript. MZ, BL and MDM investigated the SFIT4 retrieval strategy. MKS, CH, CP, TW, JMM, RK and PH provided and interpreted the TCCON data. NK and MR provided and analysed the in situ measurements. HC and RK provided the AirCore measurements. All authors read and commented the manuscript.

**Competing interests.** The authors declare that they have no conflict of interest.

**Acknowledgements.** This study is supported by the EU H2020 RINGO project. The TCCON site at Réunion Island is operated by the Royal Belgian Institute for Space Aeronomy with financial support in 2014/2015 and 2016/2017 as part of the EU project ICOS-Inwire and the ministerial decree for ICOS (FR/35/IC2), and local activities were supported by LACy/UMR8105 – Université de La Réunion. We want to thank Francis Scolas (BIRA-IASB) for maintaining the TCCON measurements at St Denis; Juha Hatakka and Tuomas Laurila (FMI) for operating the in situ and AirCore measurements at Sodankylä; Christoph Gerbig and Dietrich Feist for providing the IMECC aircraft data. We would also like to thank the TCCON network for making the data publicly available. The AirCore data from the Sodankylä site in 2017 is generated from the FRM4GHG project which received financial support from the European Space Agency under the grant agreement no. ESA-IPL-POE-LG-cl-LE-2015-1129.

**Financial support.** This research has been supported by the EU H2020 RINGO project (grant no. 730944).

**Review statement.** This paper was edited by Hartwig Harder and reviewed by two anonymous referees.

## References

- Agusti-Panareda, A., Diamantakis, M., Bayona, V., Klappenbach, F., and Butz, A.: Improving the inter-hemispheric gradient of total column atmospheric CO<sub>2</sub> and CH<sub>4</sub> in simulations with the ECMWF semi-Lagrangian atmospheric global model, *Geosci. Model Dev.*, 10, 1–18, <https://doi.org/10.5194/gmd-10-1-2017>, 2017.
- Bernath, P. F., McElroy, C. T., Abrams, M. C., Boone, C. D., Butler, M., Camy-Peyret, C., Carleer, M., Clerbaux, C., Coheur, P. F., Colin, R., DeCola, P., DeMazière, M., Drummond, J. R., Dufour, D., Evans, W. F. J., Fast, H., Fussen, D., Gilbert, K., Jennings, D. E., Llewellyn, E. J., Lowe, R. P., Mahieu, E., McConnell, J. C., McHugh, M., McLeod, S. D., Michaud, R., Midwinter, C., Nassar, R., Nichitiu, F., Nowlan, C., Rinsland, C. P., Rochon, Y. J., Rowlands, N., Semeniuk, K., Simon, P., Skelton, R., Sloan, J. J., Soucy, M. A., Strong, K., Tremblay, P., Turnbull, D., Walker, K. A., Walkty, I., Wardle, D. A., Wehrle, V., Zander, R., and Zou, J.: Atmospheric chemistry experiment (ACE): Mission overview, *Geophys. Res. Lett.*, 32, L15S01, <https://doi.org/10.1029/2005GL022386>, 2005.
- De Mazière, M., Vigouroux, C., Bernath, P. F., Baron, P., Blumenstock, T., Boone, C., Brogniez, C., Catoire, V., Coffey, M., Duchatelet, P., Griffith, D., Hannigan, J., Kasai, Y., Kramer, I., Jones, N., Mahieu, E., Manney, G. L., Piccolo, C., Randall, C., Robert, C., Senten, C., Strong, K., Taylor, J., Tétard, C., Walker, K. A., and Wood, S.: Validation of ACE-FTS v2.2 methane profiles from the upper troposphere to the lower mesosphere, *Atmos.*

- Chem. Phys., 8, 2421–2435, <https://doi.org/10.5194/acp-8-2421-2008>, 2008.
- De Mazière, M., Sha, M. K., Desmet, F., Hermans, C., Scolas, F., Kumps, N., Metzger, J.-M., Duflo, V., and Cammas, J.-P.: TCCON data from Reunion Island (RE), Release GGG2014R0, TCCON data archive, hosted by CaltechDATA, <https://doi.org/10.14291/tcon.ggg2014.reunion01.R0/1149288>, 2014.
- De Mazière, M., Thompson, A. M., Kurylo, M. J., Wild, J. D., Bernhard, G., Blumenstock, T., Braathen, G. O., Hannigan, J. W., Lambert, J.-C., Leblanc, T., McGee, T. J., Nedoluha, G., Petropavlovskikh, I., Seckmeyer, G., Simon, P. C., Steinbrecht, W., and Strahan, S. E.: The Network for the Detection of Atmospheric Composition Change (NDACC): history, status and perspectives, *Atmos. Chem. Phys.*, 18, 4935–4964, <https://doi.org/10.5194/acp-18-4935-2018>, 2018.
- Deutscher, N. M., Griffith, D. W. T., Bryant, G. W., Wennberg, P. O., Toon, G. C., Washenfelder, R. A., Keppel-Aleks, G., Wunch, D., Yavin, Y., Allen, N. T., Blavier, J.-F., Jiménez, R., Daube, B. C., Bright, A. V., Matross, D. M., Wofsy, S. C., and Park, S.: Total column CO<sub>2</sub> measurements at Darwin, Australia – site description and calibration against in situ aircraft profiles, *Atmos. Meas. Tech.*, 3, 947–958, <https://doi.org/10.5194/amt-3-947-2010>, 2010.
- Deutscher, N. M., Notholt, J., Messerschmidt, J., Weinzierl, C., Warneke, T., Petri, C., Grupe, P., and Katrynski, K.: TCCON data from Bialystok (PL), Release GGG2014R0, TCCON data archive, hosted by CaltechDATA, <https://doi.org/10.14291/tcon.ggg2014.bialystok01.R0/1149277>, 2014.
- Dils, B., Buchwitz, M., Reuter, M., Schneising, O., Boesch, H., Parker, R., Guerlet, S., Aben, I., Blumenstock, T., Burrows, J. P., Butz, A., Deutscher, N. M., Frankenberg, C., Hase, F., Hasekamp, O. P., Heymann, J., De Mazière, M., Notholt, J., Sussmann, R., Warneke, T., Griffith, D., Sherlock, V., and Wunch, D.: The Greenhouse Gas Climate Change Initiative (GHG-CCI): comparative validation of GHG-CCI SCIAMACHY/ENVISAT and TANSO-FTS/GOSAT CO<sub>2</sub> and CH<sub>4</sub> retrieval algorithm products with measurements from the TCCON, *Atmos. Meas. Tech.*, 7, 1723–1744, <https://doi.org/10.5194/amt-7-1723-2014>, 2014.
- Ehhalt, D. H. and Heidt, L. E.: Vertical profiles of CH<sub>4</sub> in the troposphere and stratosphere, *J. Geophys. Res.*, 78, 5265–5271, <https://doi.org/10.1029/JC078i024p05265>, 1973.
- European Commission: Emission Database for Global Atmospheric Research (EDGAR), release EDGARv4.2 FT2010, Tech. rep., Joint Research Centre (JRC)/Netherlands Environmental Assessment Agency (PBL), available at: <http://edgar.jrc.ec.europa.eu> (last access: 12 April 2018), 2013.
- Fraser, A., Palmer, P. I., Feng, L., Boesch, H., Cogan, A., Parker, R., Dlugokencky, E. J., Fraser, P. J., Krummel, P. B., Langenfelds, R. L., O'Doherty, S., Prinn, R. G., Steele, L. P., van der Schoot, M., and Weiss, R. F.: Estimating regional methane surface fluxes: the relative importance of surface and GOSAT mole fraction measurements, *Atmos. Chem. Phys.*, 13, 5697–5713, <https://doi.org/10.5194/acp-13-5697-2013>, 2013.
- Geibel, M. C., Messerschmidt, J., Gerbig, C., Blumenstock, T., Chen, H., Hase, F., Kolle, O., Lavrič, J. V., Notholt, J., Palm, M., Rettinger, M., Schmidt, M., Sussmann, R., Warneke, T., and Feist, D. G.: Calibration of column-averaged CH<sub>4</sub> over European TCCON FTS sites with airborne in-situ measurements, *Atmos. Chem. Phys.*, 12, 8763–8775, <https://doi.org/10.5194/acp-12-8763-2012>, 2012.
- Houweling, S., Krol, M., Bergamaschi, P., Frankenberg, C., Dlugokencky, E. J., Morino, I., Notholt, J., Sherlock, V., Wunch, D., Beck, V., Gerbig, C., Chen, H., Kort, E. A., Röckmann, T., and Aben, I.: A multi-year methane inversion using SCIAMACHY, accounting for systematic errors using TCCON measurements, *Atmos. Chem. Phys.*, 14, 3991–4012, <https://doi.org/10.5194/acp-14-3991-2014>, 2014.
- IPCC: Climate change 2013: The physical science basis. Contribution of Working Group I to the Fifth Assessment Report of the Intergovernmental Panel on Climate Change, 2013.
- Karion, A., Sweeney, C., Tans, P., and Newberger, T.: AirCore: An innovative atmospheric sampling system, *J. Atmos. Ocean. Tech.*, 27, 1839–1853, <https://doi.org/10.1175/2010JTECHA1448.1>, 2010.
- Keppel-Aleks, G., Toon, G. C., Wennberg, P. O., and Deutscher, N. M.: Reducing the impact of source brightness fluctuations on spectra obtained by Fourier-transform spectrometry., *Appl. Opt.*, 46, 4774–4779, <https://doi.org/10.1364/AO.46.004774>, 2007.
- Kilki, J., Aalto, T., Hatakka, J., Portin, H., and Laurila, T.: Atmospheric CO<sub>2</sub> observations at Finnish urban and rural sites, *Boreal Environ. Res.*, 20, 227–242, 2015.
- Kirschke, S., Bousquet, P., Ciais, P., Saunio, M., Canadell, J. G., Dlugokencky, E. J., Bergamaschi, P., Bergmann, D., Blake, D. R., Bruhwiler, L., Cameron-Smith, P., Castaldi, S., Chevallier, F., Feng, L., Fraser, A., Heimann, M., Hodson, E. L., Houweling, S., Josse, B., Fraser, P. J., Krummel, P. B., Lamarque, J.-F., Langenfelds, R. L., Le Quééré, C., Naik, V., O'Doherty, S., Palmer, P. I., Pison, I., Plummer, D., Poulter, B., Prinn, R. G., Rigby, M., Ringeval, B., Santini, M., Schmidt, M., Shindell, D. T., Simpson, I. J., Spahni, R., Steele, L. P., Strode, S. A., Sudo, K., Szopa, S., van der Werf, G. R., Voulgarakis, A., van Weele, M., Weiss, R. F., Williams, J. E., and Zeng, G.: Three decades of global methane sources and sinks, *Nat. Geosci.*, 6, 813–823, <https://doi.org/10.1038/ngeo1955>, 2013.
- Kivi, R., Heikkinen, P., and Kyrö, E.: TCCON data from Sodankyla (FI), Release GGG2014R0, TCCON data archive, hosted by CaltechDATA, <https://doi.org/10.14291/tcon.ggg2014.sodankyla01.R0/1149280>, 2014.
- Notholt, J., Petri, C., Warneke, T., Deutscher, N. M., Buschmann, M., Weinzierl, C., Macatangay, R., and Grupe, P.: TCCON data from Bremen (DE), Release GGG2014R0, TCCON data archive, hosted by CaltechDATA, <https://doi.org/10.14291/tcon.ggg2014.bremen01.R0/1149275>, 2014.
- Notholt, J., Warneke, T., Petri, C., Deutscher, N. M., Weinzierl, C., Palm, M., and Buschmann, M.: TCCON data from Ny Ålesund, Spitsbergen (NO), Release GGG2014.R0, TCCON data archive, hosted by CaltechDATA, <https://doi.org/10.14291/tcon.ggg2014.nyalesund01.R0/1149278>, 2017.
- Ostler, A., Sussmann, R., Patra, P. K., Houweling, S., De Bruine, M., Stiller, G. P., Haenel, F. J., Plieninger, J., Bousquet, P., Yin, Y., Saunio, M., Walker, K. A., Deutscher, N. M., Griffith, D. W. T., Blumenstock, T., Hase, F., Warneke, T., Wang, Z., Kivi,



- R., and Robinson, J.: Evaluation of column-averaged methane in models and TCCON with a focus on the stratosphere, *Atmos. Meas. Tech.*, 9, 4843–4859, <https://doi.org/10.5194/amt-9-4843-2016>, 2016.
- Pougatchev, N. S., Connor, B. J., and Rinsland, C. P.: Infrared measurements of the ozone vertical distribution above Kitt Peak, *J. Geophys. Res.*, 100, 16689, <https://doi.org/10.1029/95JD01296>, 1995.
- Rigby, M., Prinn, R. G., Fraser, P. J., Simmonds, P. G., Langenfelds, R. L., Huang, J., Cunnold, D. M., Steele, L. P., Krummel, P. B., Weiss, R. F., O'Doherty, S., Salameh, P. K., Wang, H. J., Harth, C. M., Mühle, J., and Porter, L. W.: Renewed growth of atmospheric methane, *Geophys. Res. Lett.*, 35, L22805, <https://doi.org/10.1029/2008GL036037>, 2008.
- Rodgers, C. D.: *Inverse Methods for Atmospheric Sounding – Theory and Practice*, Series on Atmospheric Oceanic and Planetary Physics, vol. 2, World Scientific Publishing Co. Pte. Ltd, Singapore, <https://doi.org/10.1142/9789812813718>, 2000.
- Rodgers, C. D.: Intercomparison of remote sounding instruments, *J. Geophys. Res.*, 108, 46–48, <https://doi.org/10.1029/2002JD002299>, 2003.
- Rothman, L. S., Gordon, I. E., Babikov, Y., Barbe, A., Chris Benner, D., Bernath, P. F., Birk, M., Bizzocchi, L., Boudon, V., Brown, L. R., Campargue, A., Chance, K., Cohen, E. A., Coudert, L. H., Devi, V. M., Drouin, B. J., Fayt, A., Flaud, J. M., Gamache, R. R., Harrison, J. J., Hartmann, J. M., Hill, C., Hodges, J. T., Jacquemart, D., Jolly, A., Lamouroux, J., Le Roy, R. J., Li, G., Long, D. A., Lyulin, O. M., Mackie, C. J., Massie, S. T., Mikhailenko, S., Müller, H. S. P., Naumenko, O. V., Nikitin, A. V., Orphal, J., Perevalov, V., Perrin, A., Polovtseva, E. R., Richard, C., Smith, M. A. H., Starikova, E., Sung, K., Tashkun, S., Tennyson, J., Toon, G. C., Tyuterev, V. G., and Wagner, G.: The HITRAN2012 molecular spectroscopic database, *J. Quant. Spectrosc. Rad.*, 130, 4–50, <https://doi.org/10.1016/j.jqsrt.2013.07.002>, 2013.
- Saad, K. M., Wunch, D., Toon, G. C., Bernath, P., Boone, C., Connor, B., Deutscher, N. M., Griffith, D. W. T., Kivi, R., Notholt, J., Roehl, C., Schneider, M., Sherlock, V., and Wennberg, P. O.: Derivation of tropospheric methane from TCCON CH<sub>4</sub> and HF total column observations, *Atmos. Meas. Tech.*, 7, 2907–2918, <https://doi.org/10.5194/amt-7-2907-2014>, 2014.
- Saad, K. M., Wunch, D., Deutscher, N. M., Griffith, D. W. T., Hase, F., De Mazière, M., Notholt, J., Pollard, D. F., Roehl, C. M., Schneider, M., Sussmann, R., Warneke, T., and Wennberg, P. O.: Seasonal variability of stratospheric methane: implications for constraining tropospheric methane budgets using total column observations, *Atmos. Chem. Phys.*, 16, 14003–14024, <https://doi.org/10.5194/acp-16-14003-2016>, 2016.
- Saito, R., Patra, P. K., Deutscher, N., Wunch, D., Ishijima, K., Sherlock, V., Blumenstock, T., Dohe, S., Griffith, D., Hase, F., Heikkinen, P., Kyrö, E., Macatangay, R., Mendonca, J., Messerschmidt, J., Morino, I., Notholt, J., Rettinger, M., Strong, K., Sussmann, R., and Warneke, T.: Technical Note: Latitude-time variations of atmospheric column-average dry air mole fractions of CO<sub>2</sub>, CH<sub>4</sub> and N<sub>2</sub>O, *Atmos. Chem. Phys.*, 12, 7767–7777, <https://doi.org/10.5194/acp-12-7767-2012>, 2012.
- Schmidt, M., Lopez, M., Yver Kwok, C., Messenger, C., Ramonet, M., Wastine, B., Vuillemin, C., Truong, F., Gal, B., Parmentier, E., Cloué, O., and Ciais, P.: High-precision quasi-continuous atmospheric greenhouse gas measurements at Trainou tower (Orléans forest, France), *Atmos. Meas. Tech.*, 7, 2283–2296, <https://doi.org/10.5194/amt-7-2283-2014>, 2014.
- Sheese, P. E., Boone, C. D., and Walker, K. A.: Detecting physically unrealistic outliers in ACE-FTS atmospheric measurements, *Atmos. Meas. Tech.*, 8, 741–750, <https://doi.org/10.5194/amt-8-741-2015>, 2015.
- Tikhonov, A. N.: Solution of Incorrectly Formulated Problems and the Regularisation Method, *Soviet. Math. Dokl.*, 4, 1035–1038, <https://doi.org/10.1111/J.1365-246X.2012.05699.X>, 1963.
- Toon, G. C.: Telluric line list for GGG2014, TCCON data archive, hosted by the Carbon Dioxide Information Analysis Center, Oak Ridge National Laboratory, Oak Ridge, Tennessee, USA, <https://doi.org/10.14291/tcon.ggg2014.atm.R0/1221656>, 2014.
- Tukiainen, S., Railo, J., Laine, M., Hakkarainen, J., Kivi, R., Heikkinen, P., Chen, H., and Tamminen, J.: Retrieval of atmospheric CH<sub>4</sub> profiles from Fourier transform infrared data using dimension reduction and MCMC, *J. Geophys. Res.-Atmos.*, 121, 10312–10327, <https://doi.org/10.1002/2015JD024657>, 2016.
- Wang, Z., Deutscher, N. M., Warneke, T., Notholt, J., Dils, B., Griffith, D. W. T., Schmidt, M., Ramonet, M., and Gerbig, C.: Retrieval of tropospheric column-averaged CH<sub>4</sub> mole fraction by solar absorption FTIR-spectrometry using N<sub>2</sub>O as a proxy, *Atmos. Meas. Tech.*, 7, 3295–3305, <https://doi.org/10.5194/amt-7-3295-2014>, 2014.
- Wang, Z., Warneke, T., Deutscher, N. M., Notholt, J., Karstens, U., Saunio, M., Schneider, M., Sussmann, R., Sembhi, H., Griffith, D. W. T., Pollard, D. F., Kivi, R., Petri, C., Velasco, V. A., Ramonet, M., and Chen, H.: Contributions of the troposphere and stratosphere to CH<sub>4</sub> model biases, *Atmos. Chem. Phys.*, 17, 13283–13295, <https://doi.org/10.5194/acp-17-13283-2017>, 2017.
- Warneke, T., Messerschmidt, J., Notholt, J., Weinzierl, C., Deutscher, N. M., Petri, C., Grupe, P., Vuillemin, C., Truong, F., Schmidt, M., Ramonet, M., and Parmentier, E.: TCCON data from Orléans (FR), Release GGG2014R0, TCCON data archive, hosted by CaltechDATA, <https://doi.org/10.14291/tcon.ggg2014.orleans01.R0/1149276>, 2014.
- Waymark, C., Waymark, C., Walker, K., Boone, C. D., and Bernath, P. F.: ACE-FTS version 3.0 data set: validation and data processing update, *Ann. Geophys.*, 56, <https://doi.org/10.4401/ag-6339>, 2014.
- Wunch, D., Toon, G. C., Blavier, J.-F. L., Washenfelder, R. A., Notholt, J., Connor, B. J., Griffith, D. W. T., Sherlock, V., and Wennberg, P. O.: The Total Carbon Column Observing Network, *Philos. Trans. R. Soc. A Math. Phys. Eng. Sci.*, 369, 2087–2112, <https://doi.org/10.1098/rsta.2010.0240>, 2011.
- Wunch, D., Toon, G. C., Sherlock, V., Deutscher, N. M., Liu, C., Feist, D. G., and Wennberg, P. O.: The Total Carbon Column Observing Network's GGG2014 Data Version, p. 43, <https://doi.org/10.14291/tcon.ggg2014.documentation.R0/1221662>, 2015.
- Wunch, D., Toon, G. C., Hedelius, J. K., Vizenor, N., Roehl, C. M., Saad, K. M., Blavier, J.-F. L., Blake, D. R., and Wennberg, P. O.: Quantifying the loss of processed natural gas within California's South Coast Air Basin using long-term measurements of ethane and methane, *Atmos. Chem. Phys.*, 16, 14091–14105, <https://doi.org/10.5194/acp-16-14091-2016>, 2016.

- Yang, Z., Toon, G. C., Margolis, J. S., and Wennberg, P. O.: Atmospheric CO<sub>2</sub> retrieved from ground-based near IR solar spectra, *Geophys. Res. Lett.*, 29, 1–4, <https://doi.org/10.1029/2001GL014537>, 2002.
- Zhou, M., Dils, B., Wang, P., Detmers, R., Yoshida, Y., O'Dell, C. W., Feist, D. G., Velazco, V. A., Schneider, M., and De Mazière, M.: Validation of TANSO-FTS/GOSAT XCO<sub>2</sub> and XCH<sub>4</sub> glint mode retrievals using TCCON data from near-ocean sites, *Atmos. Meas. Tech.*, 9, 1415–1430, <https://doi.org/10.5194/amt-9-1415-2016>, 2016.
- Zhou, M., Langerock, B., Vigouroux, C., Sha, M. K., Ramonet, M., Delmotte, M., Mahieu, E., Bader, W., Hermans, C., Kumps, N., Metzger, J.-M., Dufflot, V., Wang, Z., Palm, M., and De Mazière, M.: Atmospheric CO and CH<sub>4</sub> time series and seasonal variations on Reunion Island from ground-based in situ and FTIR (NDACC and TCCON) measurements, *Atmos. Chem. Phys.*, 18, 13881–13901, <https://doi.org/10.5194/acp-18-13881-2018>, 2018.